ELSEVIER

Polymer 42 (2001) 8857–8865

polymer

www.elsevier.com/locate/polymer

Synergistic toughening effect of SBS and HDPE on the fracture of the PS/HDPE/SBS blends

Jingshen Wu[a,*], Baohua Guo[b], Chi-Ming Chan[b], Jianxiong Li[b], Hoi-Shuen Tang[a]

[a]*Department of Mechanical Engineering, The Hong Kong University of Science and Technology, Clear Water Bay, Kowloon, Hong Kong*
[b]*Department of Chemical Engineering, The Hong Kong University of Science and Technology, Clear Water Bay, Kowloon, Hong Kong*

Received 27 December 2000; received in revised form 9 February 2001; accepted 12 March 2001

Abstract

The microstructure and mechanical properties of the blends consisting of polystyrene and high-density polyethylene and/or styrene–butadiene–styrene were studied. The HDPE forms long fibers in both the PS/HDPE and PS/HDPE/SBS blends. The binary blends exhibit declined mechanical properties at all compositions. Mechanism study suggests that craze formation in PS followed by unstable crack propagation along the weak PS–HDPE interface is the major failure mechanism for the low impact strength of the binary blends. In the ternary blends, the SBS forms a thin layer covering the HDPE fibers, which improves the PS–HDPE interfacial strength and mechanical properties of the blends. The debonding-cavitation at the PS–HDPE interface releases the plastic constraint and enables shear deformation at the crack tip. Moreover, the HDPE-fiber-pullout promotes shear deformation of PS. Both mechanisms greatly improve the toughness of the ternary blends.

Keywords: PS/HDPE/SBS blends; Interfacial adhesion; Fracture mechanisms

1. Introduction

Toughening brittle polymers through blending with rubbery polymers has been studied extensively in the past decades. A large number of toughened polymer systems, such as high impact polystyrene (HIPS) and epoxy/rubber blends, has been developed and employed widely as engineering materials [1]. Toughening mechanism study on these systems shows that the rubbery component in the blends can effectively initiate and promote certain energy dissipating processes, e.g. massive crazing [1,2], cavitation [3–9], crack bridging [10,11], shear banding [12–14] and matrix shear yielding [15–18], in polymer matrices. Consequently, both crack initiation and propagation resistance can be substantially increased.

On the other hand, the improvement in fracture toughness for the traditional rubber-toughened polymer blends is achieved, in most cases, at the cost of other important mechanical properties. For instance, rubber toughened polymer blends generally have a much lower elastic modulus and yield strength compared with their corresponding homopolymers. This drawback has greatly limited the use of the rubber-toughened blends in certain engineering applications, where high modulus, yield strength and toughness are essential. To overcome this problem, inorganic rigid particles, such as calcium carbonate, glass beads and barium sulphate, have been used to toughen brittle polymers and achieved some success [19,20]. However, the major difficulties facing this particular system are the limited enhancement in toughness (especially at low temperature) and reduced processing windows due to viscosity increase.

Toughening brittle polymers by addition of rigid polymer components is a relatively new concept in polymer toughening. It has been practiced in the past few years and several rigid–rigid polymer systems have been developed and investigated; among them are polyamide/polyphenylene oxide (PA/PPO) [9], polybutylene terephthalate/polycarbonate (PBT/PC) [21–23], polyethylene terephthalate/polycarbonate (PET/PC) [24–29], polycarbonate/polymethyl methacrylate (PC/PMMA) [30], polyamide-6/poly(*m*-xylene adipamide) (PA6/MXD6) [31], polystyrene/polymethyl methacrylate (PS/PMMA) [32] and polystyrene/polyethylene (PS/PE) [33–35]. The results of the studies show that it is possible to toughen brittle polymers by the use of another rigid polymer component. The toughness of the resultant rigid–rigid polymer blends may be substantially enhanced without scarifying other mechanical properties. The key factor to achieve this goal is that the rigid–rigid polymer blends must have a well-tailored microstructure, especially

* Corresponding author. Tel.: +852-2358-7200; fax: +852-2358-1543.
E-mail address: mejswu@ust.hk (J.S. Wu).

0032-3861/01/$ - see front matter
PII: S0032-3861(01)00443-8

the interfacial condition, to initiate and promote necessary toughening events during the fracture of the blends.

PS is one of the most extensively studied brittle polymers regarding to toughening. Various rubbery components have been used and toughening mechanisms have been studied. It is now generally accepted [1] that the rubber particles in the PS/rubber blends work as stress concentrators to initiate a massive number of crazes in the PS matrix. The crazes will keep growing in the direction perpendicular to the principal applied stress until they encounter and are stabilized by the neighboring rubber particles. A large amount of energy consumed in craze initiation and development is the major source of toughness. Similar to the other rubber toughened polymer blends, the major drawback of the PS/rubber blends is the reduced modulus and yield strength. In recent years, attempts to toughen PS using non-rubbery polymers have been made. Polyethylene (PE) is one of the polymers frequently used in PS blends [33–35]. Since PS and PE are immiscible polymers, simple mixing of the two components very often leads to a PS/PE mixture with very poor mechanical properties. Hence, research efforts have been made in the past to compatibilize the system to improve its mechanical properties. The most popular way of compatibilization is to apply a third component, in many cases, a copolymer, during the processing of the blends. For the PS/PE system, copolymers such as SEBS [36–38], PE–PS copolymer [39] and other copolymers [40], were used to compatibilize the system and enhanced its toughness. In the present work, toughening PS by blending it with HDPE was evaluated. A styrene–butadiene–styrene (SBS) copolymer was adopted as the compatibilizer in the blending of the PS and HDPE. The microstructure and mechanical properties of the PS/HDPE blends with and without SBS were reported. The mechanisms responsible for the observed synergistic effect of the HDPE and SBS on toughening of the PS were discussed and proposed.

2. Experimental

2.1. Raw materials and blends preparation

PS from Dow Chemical was used in our study. The HDPE used in the current study was obtained from Philips Petroleum Ltd (HMMPE). The SBS copolymer was kindly supplied by Yueyang Petrochemical Co. China (SBS-791). The specifications of the raw materials are listed in Table 1. The number-average and weight-average molecular weights of the HDPE were measured with a high-temperature gel permeation chromatography (GPC) system (Waters 150C). The HDPE was dissolved in 1,2,4-tricholobenzene at 160°C. The molecular weights of the PS and SBS were tested with a regular GPC. The weight percentage of PS- and PB- blocks in the SBS was determined by NMR.

The PS/HDPE/SBS blends were prepared using a Haake Rheocord mixer 9000 by a two-step mixing method [33]. In the first step, the weighted PS and HDPE pellets were premixed at 165–175°C for about 5 min. In the second step, the resultant PS/HDPE pre-blend was mixed with the weighted SBS pellets in the same mixer at the same temperature for about 5 min. A stabiliser (Irganox 1010) was used during the second step mixing. The obtained PS/HDPE/SBS blends were dried and injection moulded into standard testing specimens at 220–260°C.

2.2. Mechanical tests

The tensile and Izod impact tests were conducted according to ASTM D250 and D638, respectively. The former was done on an Instron machine (Model 5567) at a crosshead speed of 20 mm/min. and the latter was performed on a Tinius Olsen impact tester (Model 92T) with V-notched specimens. For both tensile and impact tests, at least six samples were used for each measurement. The average of six values was used in the subsequent analysis.

2.3. Morphology and fracture mechanism study

The morphology of the blends was disclosed using a transmission electron microscope (TEM) and a scanning electron microscope (SEM). In the TEM study, ultra-thin sections of 60–80 nm were cut using a Reichert-Jung Ultracut R microtome. In the fracture mechanism study, ultra-thin sections containing an arrested crack tip were used. The plane of the thin sections was perpendicular to the crack plane. The schematic of the TEM sampling process for fracture mechanism study is illustrated in Fig. 1 and more information on the TEM sample preparation can be found in two previous papers of the authors [10,41]. To enhance the contrast of the TEM image, the thin sections were stained by RuO_4 at room temperature before they were examined under a JOEL JEM-100CX transmission electron microscope. The details on the staining technique can also be found in our earlier work [10,41].

The SEM samples for morphology and fracture mechanism studies were directly taken from the broken pieces after the impact test. The fracture surface was coated with a thin

Table 1
Specification of the raw materials used in the current study

Material code	$\bar{M}_n$ ($\times 10^4$)	$\bar{M}_w$ ($\times 10^5$)	wt% of PS	$\bar{M}_n$ (PS block) ($\times 10^3$)	$\bar{M}_n$ (PB block) ($\times 10^5$)
HMMPE	2.04	1.45			
PS	9.29	2.97			
SBS-791	5.67	1.53	30	8.51	3.97

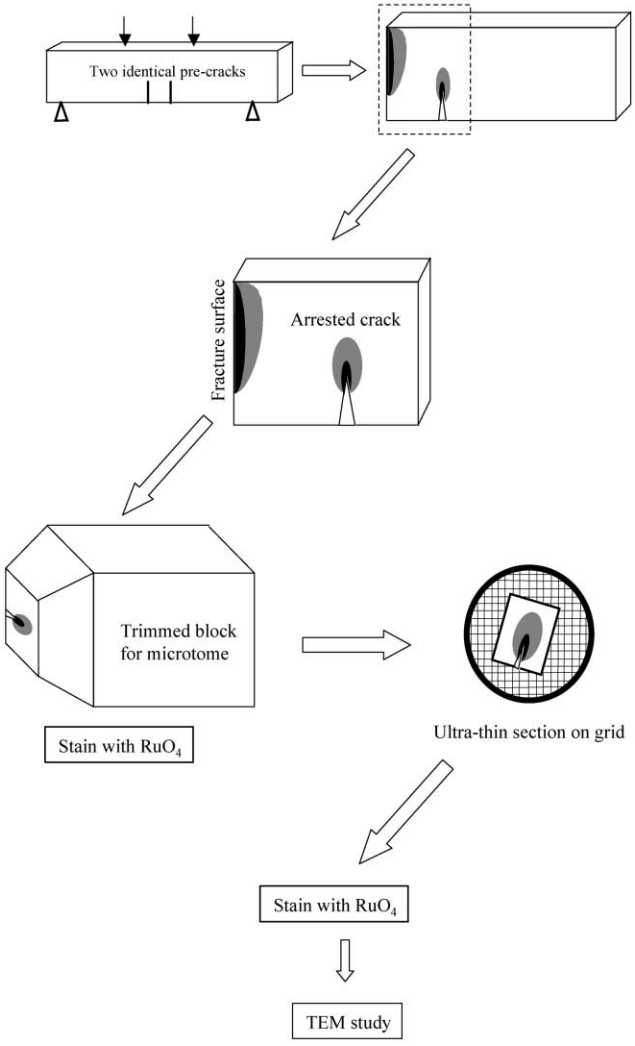

Fig. 1. Schematic of the TEM sample preparation process for the toughening mechanism study.

layer of gold of approximately 200 Å in thickness, before it was observed in a JEOL 6300M scanning electron microscope. Toluene was used to extract PS and SBS from the PS/HDPE/SBS blends to better reveal the microstructure. The extraction was conducted at room temperature for about 48 h. The toluene-treated samples were dried at 70°C for 24 h before gold coating and SEM observation.

3. Results and discussion

3.1. Microstructure of the binary and ternary blends

A TEM micrograph taken from a PS/SBS (90/10) blend is shown in Fig. 2. Due to the low concentration of the SBS and the high miscibility between the two components, the SBS is uniformly distributed as very fine particles in the PS matrix. The average size of the SBS particles is about 100–200 nm long and less than 50 nm wide. An immediate

Fig. 2. TEM micrograph of the PS/SBS (90/10) binary blend stained with RuO_4. The small black particles are SBS domains.

impression from this TEM observation is that the particles are most likely too small to toughen PS. According to the well-established toughening mechanisms [1,15–17,42], the small SBS particles can effectively initiate crazes in the PS matrix; however, they are too small to stop the growing of the crazes into harmful cracks, leading to low fracture toughness. This prediction was confirmed by the results of our toughness tests, as will be discussed in a later section.

Fig. 3 is a SEM micrograph taken from a PS/HDPE (80/20) blend after a 48 h toluene extraction. It clearly demonstrates that the blend has a fiber-like HDPE phase and a continuous PS matrix, which had been extracted by toluene. The diameter of the fibers ranges from 0.5 to 5 μm. The length of the fibers is substantial, which reflects that the size of the HDPE droplets was very large before they were converted into fibers during injection molding. Since the size of dispersed phase is an indication of the compatibility between the dispersed phase and matrix, the long HDPE fibers imply a low compatibility between the HDPE and

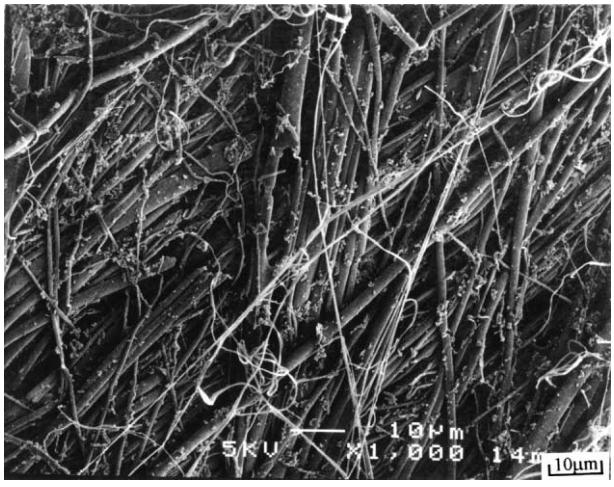

Fig. 3. SEM micrograph of the PS/HDPE (80/20) binary blend after 48 h toluene extraction. HDPE fibers are clearly seen.

Fig. 4. Enlargement of Fig. 3 showing the detailed surface condition of the HDPE fibers.

PS. Additional evidence supportive to this conclusion was obtained in an enlarged SEM micrograph of the PS/HDPE blend shown in Fig. 4. Evidently, the surface of the HDPE fibers is clean. There is no sign showing that the bonding between the PS and HDPE was strong.

The addition of 10 wt% of SBS into the PS/HDPE blend resulted in a unique microstructure. A SEM micrograph of the PS/HDPE/SBS ternary blend is shown in Fig. 5. Apparently, the HDPE is in a string-and-beads structure. Many elliptical HDPE particles are linked together by very thin HDPE fibrils. The size of the elliptical particles is around 2–5 μm. The TEM micrograph of the ternary blend in Fig. 6 revealed that the SBS forms a thin interfacial layer between the HDPE phase and the PS matrix. Since the S-block of SBS has a high miscibility with the PS and the B-block is compatible with HDPE, the SBS component functions as a surfactant and reduces substantially the surface tension of

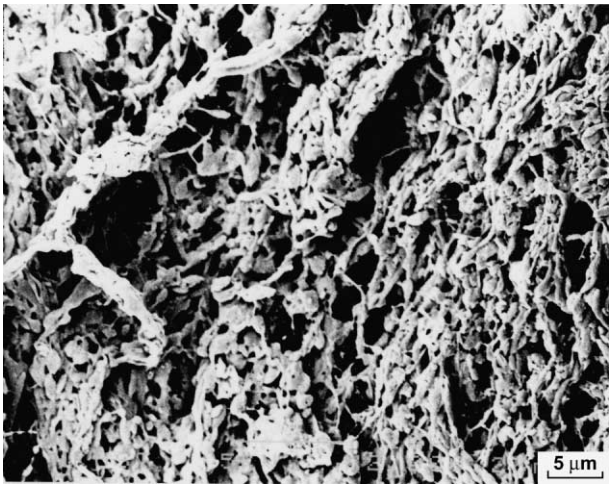

Fig. 5. SEM micrograph of the PS/HDPE/SBS (72/18/10) ternary blend after 48 h toluene extraction. The HDPE fibers are in a string-and-beads structure.

Fig. 6. TEM micrograph of the PS/HDPE/SBS (72/18/10) ternary blend stained with RuO_4. It is clearly seen that the SBS (the darkest phase) formed a thin layer covering the HDPE fibers.

the HDPE in PS. As a result, the compatibility between the HDPE and PS is improved. The detailed mechanisms of the formation and evolution of the interface under different thermal conditions have been reported [43].

3.2. Mechanical properties of the binary blends

3.2.1. PS/HDPE Blends

The results of the mechanical tests of the PS/HDPE blends are shown in Table 2. It is clear that simple mixing of PS with HDPE has a negative impact on the mechanical properties of the blends. For example, the tensile strength decreased from about 61.50 to 49.60 MPa when 20 wt% HDPE was added. Meanwhile, the Young's modulus and elongation at break decreased with the HDPE content, too. The former dropped from 3.86 to 2.90 GPa and the latter from 4.90 to 3.58%. Fig. 7 shows the variation of the impact strength versus the HDPE content. It has a typical profile for incompatible polymer blends. The large scatter of the data points indicates that flaws, due to the low miscibility of PS and HDPE, exist in the samples, which make the quality and mechanical integrity of the blends fluctuate from specimen to specimen.

A careful examination on the fracture surface of the PS/HDPE blends (Fig. 8) revealed that: (1) the continuous phase (PS) fractured in a brittle mode with very little plastic deformation. The area between the neighboring fibers features a dimple-like structure that has a relatively large and smooth center and a thin, stress-whitened circular edge. (2) There are many holes, fiber ends and, highly deformed and broken fibrils on the fracture surface. The holes were obviously formed by the HDPE-fiber-pullout process during crack opening. It is conceivable that the fiber ends corresponding to the holes can be found on the surface of the other half of the broken sample. (3) There is a large space between the highly elongated fibrils and the surrounding matrix. This observation suggests that lateral contraction of the HDPE fibers occurred due to its elongation along

Table 2
Mechanical properties of the binary and ternary blends used in the present study

Composition		Tensile strength (MPa)		Young's modulus (GPa)		Elongation at break (%)		Impact strength (J/m)	
		PS/HDPE	PS/HDPE/SBS(10%)	PS/HDPE	PS/HDPE/SBS(10%)	PS/HDPE	PS/HDPE/SBS	PS/HDPE	PS/HDPE/SBS(10%)
HDPE (wt%)	0	61.50	55.80	3.86	2.92	4.90	3.00	22.90	20.90
	5	60.70	53.50	3.60	2.83	4.90	13.20	11.20	66.30
	7	61.40	/	3.27	/	4.90	/	18.50	/
	8.5	60.60	/	3.20	/	5.00	/	15.60	/
	10	57.80	/	3.13	/	4.60	/	11.40	/
	15	52.00	/	2.93	/	3.70	/	12.00	/
	20	49.60	44.50	2.90	2.53	3.58	77.50	16.10	201.31
Composition		PS/SBS	PS/HDPE/SBS[a]	PS/SBS	PS/HDPE/SBS[a]	PS/SBS	PS/HDPE/SBS[a]	PS/SBS	PS/HDPE/SBS[1]
SBS (wt%)	0	61.40	61.50	3.86	3.27	5.00	3.16	23.10	16.67
	5	53.20	59.50	3.32	3.34	3.98	12.13	21.54	72.70
	10	49.00	52.90	3.04	2.75	7.97	77.32	21.00	185.00
	15	43.20	44.50	2.73	2.69	14.14	79.69	20.12	301.00

[a] PS:HDPE = 4:1

the fiber direction under tension. The constraint of the matrix to the fiber lateral contraction seems negligible, as there is little matrix deformation can be seen. This finding confirms that the adhesive between the HDPE fibers and the matrix is poor.

Given the fractographic observation discussed above, the failure mechanism of the PS/HDPE blends may be proposed as follows. When the PS/HDPE sample is loaded, crazes are formed in the PS matrix. The crazes then grow in a direction perpendicular to the applied stress. In a later stage, they develop into micro-cracks under further loading. The stress level at the crack tip is high and increases rapidly with the applied load. When the stress level at crack tip exceeds the fracture strength of the PS, the ligament between the HDPE fibers will fracture in a brittle manner, resulting in a smooth fracture surface. The stress-whitened circular edge is formed in the last stage of the micro-crack propagation, because at that moment, the remaining of the ligament is extremely thin and may fracture under plane-stress condition. For those long fibers bridging across the propagating cracks, though the fiber-matrix interfacial bonding is poor, the mechanical interlock between the fiber and matrix will prevent the fiber from pullout. Thus, the long fibers will be stretched into thin fibrils during the crack-opening process and, eventually, broken down after extensive elongation. The bridging effect of this part of HDPE fibers is beneficial to the fracture toughness of the blends. However, the number of these bridging fibers is few and the overall contribution from these fibers to the toughness of the blends is not significant.

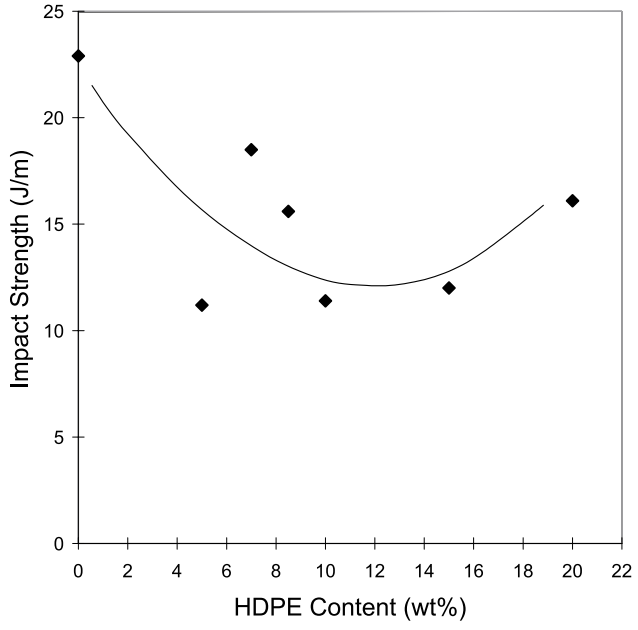

Fig. 7. Variation of the impact strength against the HDPE content obtained with the PS/HDPE binary blends.

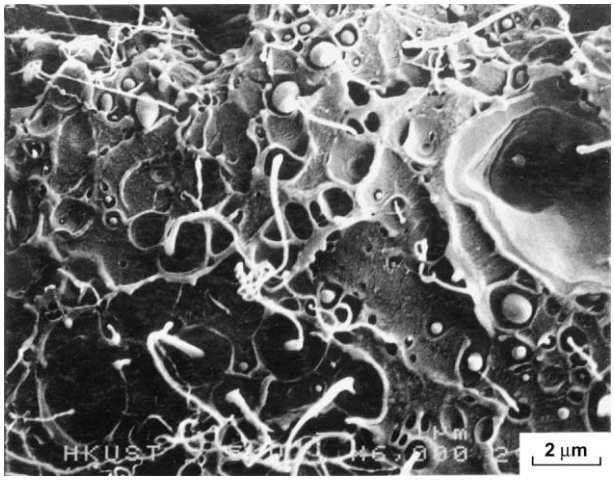

Fig. 8. SEM micrograph of the fracture surface of the PS/HDPE (80/20) binary blend. Elongated HDPE fibers, deformed fiber ends and holes due to fiber pullout are clearly seen.

3.2.2. PS/SBS Blends

As expected, addition of soft SBS to rigid PS matrix softens the matrix. As demonstrated by Table 2, the tensile strength and Young's modulus of the PS/SBS blends decreases with increase of the SBS content. After 15 wt% SBS was added, the Young's modulus of the blends decreased from 3.27 to 2.69 GPa and the tensile strength dropped from 61.40 to 43.20 MPa. However, it is interesting to note that although the elongation at break (ductility) increases substantially from ~5 to 14% after addition of 15 wt% SBS, the impact strength of the blends decreases (see Fig. 9). If we recall that the miscibility of the PS and SBS is high and the particle size of the SBS in PS is extremely small (cf. Fig. 2), this seemingly contradictory phenomenon of low impact strength at high ductility is not difficult to understand.

It is well known that the crazing stress of PS is lower than its shear yielding stress, thus, PS has a strong tendency to form crazes when it is loaded under plane-strain condition. In toughening of PS, introducing massive crazes into PS by addition of rubber particle is the major toughening strategy [1]. For the massive crazing mechanism to work, the rubber particles must serve as stress concentrators to initiate massive crazes to dissipate fracture energy, and meanwhile, they must also act as stabilizers to stop the growing crazes and prevent the crazes from developing into harmful cracks. To be a stabilizer, the rubber particle must have a relatively large particle size. Previous research results have demonstrated that stabilization from the rubber particles smaller than 1 μm is negligible and the optimum particle size for maximum toughness in PS ranges from 1 to 4 μm [44,45].

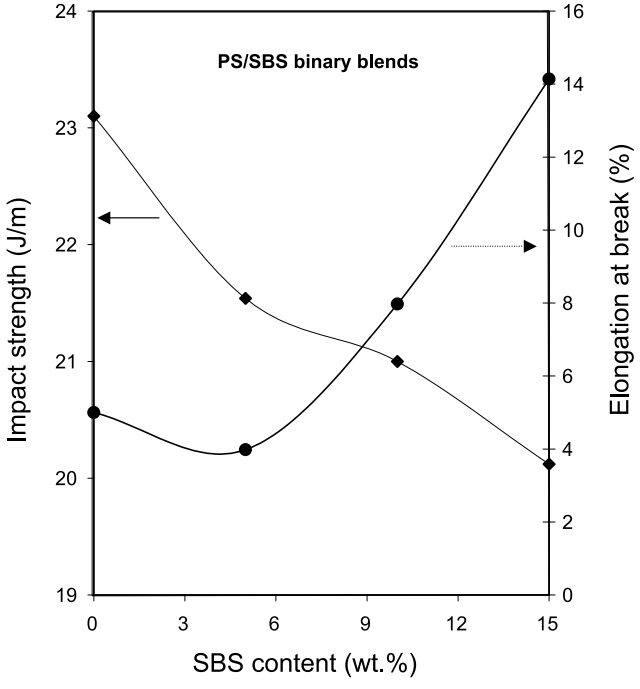

Fig. 9. Variation of the impact strength and elongation at break against the SBS content obtained with the PS/SBS binary blends.

The crazes initiated by very small rubber particles can easily develop into cracks, leading to catastrophic fracture with very low toughness.

Since the particle size of the SBS in the present PS/SBS blends is in the range of 50–100 nm, it is by far too small to stabilize growing crazes. When the notched PS/SBS specimen was tested under impact loading, the material in front of the crack tip was subjected to a high plastic constraint. The tri-axial tensile stress field would promote the craze formation at the equators of the SBS rubber particles [15]. Once the crazes were formed, the growing crazes would soon develop into cracks, because the particle was too small to stabilize the crazes, and lead to brittle failure of the specimen with low toughness. On the other hand, when the PS/SBS blends were tested under uniaxial tension, where plane-stress is the dominant stress condition, the very fine SBS particles worked as a plasticizer and enhanced the mobility and relative movement of the PS chains under shearing. The enhanced inter- and intra-molecular movements would render the PS/SBS blends with high ductility under tension.

3.3. Mechanical properties of the ternary blends

As discussed in the above section, blending PS with either HDPE or SBS cannot achieve the anticipated improvement in the mechanical properties, especially, fracture toughness. In fact, negative blending effect was observed. The causes of the negative blending effect for the PS/HDPE are the low compatibility and poor interfacial adhesion between the two components. In contrast to the PS/HDPE blend, the failure of the PS/SBS blend was caused by the high compatibility between PS and SBS. The dispersed SBS particles were too small to stabilize the growing crazes. It is, therefore, a natural consideration that the combination of the two binary systems at an appropriate composition may bring about a ternary blend with a proper microstructure and the required synergistic toughening effect.

Indeed, when the three components were blended together, both ductility and impact strength of the ternary blends were improved dramatically. For example, when 10wt% SBS was added into the PS/HDPE system, the impact strength of the PS/HDPE/SBS blends increased linearly with the HDPE content from ~21 to 201 J/m. At the meantime, the ductility of the blends also increased from 3 to ~77%. At a fixed PS/HDPE ratio (4:1), the impact strength of the PS/HDPE/SBS blends increased with the SBS content even more substantially. With 15 wt% SBS added, the impact strength of the ternary blend is about 301 J/m, which is 15 times of the PS/HDPE binary blend. The ductility of the blends was also improved markedly. The mechanical properties of the ternary blends are summarized in Table 2.

The fractography of the ternary blends revealed that the toughening mechanism involved in the fracture of the PS/HDPE/SBS ternary blends was not the massive crazing

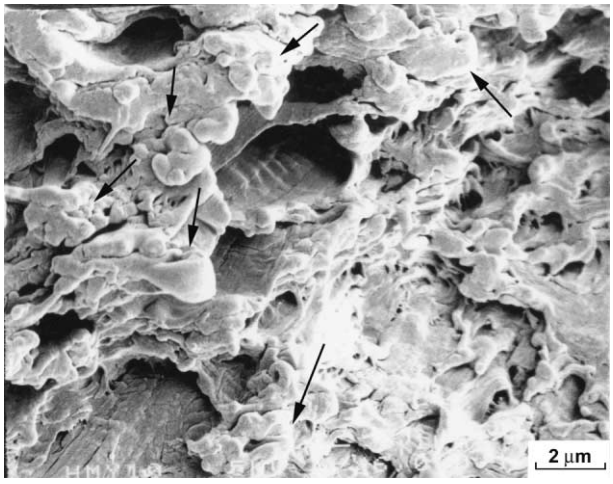

Fig. 10. SEM micrograph of the fracture surface of the PS/HDPE/SBS (72/18/10) ternary blend after impact test.

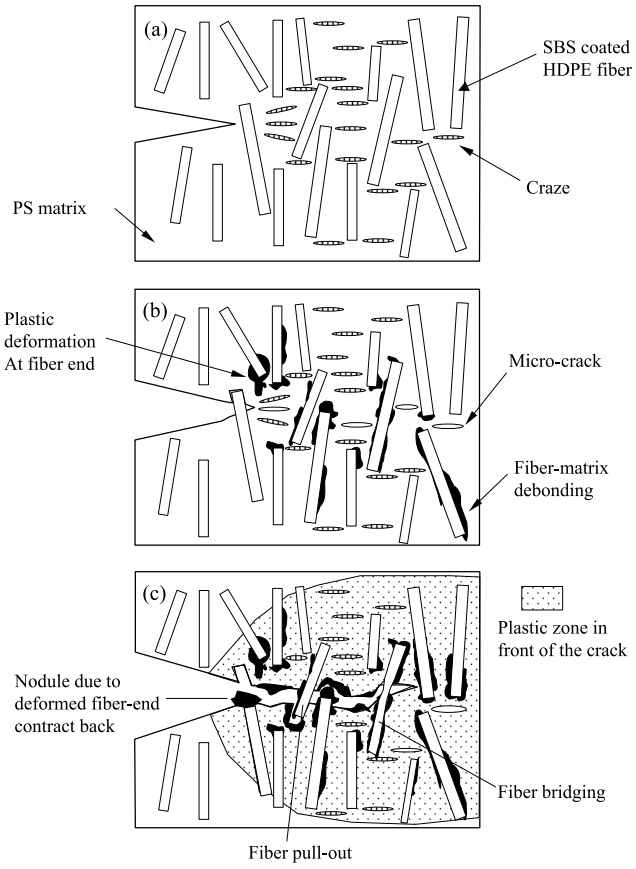

Fig. 11. Schematic picture describing the toughening events observed during the fracture process of the toughened PS/HDPE/SBS ternary blends.

mechanism, as it would normally expect for PS based blends. As demonstrated by a SEM micrograph taken from the fracture surface of a PS/HDPE/SBS blend (Fig. 10), the observed high toughness was actually caused by large-scale shear deformation of the PS and HDPE phases. As discussed in the previous section, since the crazing stress of PS is much lower than its shear yielding stress, craze will form prior to shear yielding when a PS sample is loaded under plane-strain condition. During the fracture of the blends with PS as the matrix, shear deformation is generally unexpected, unless it is promoted by other mechanisms. A closer examination on Fig. 10 discloses that there are many deformed holes and nodular structures on the fracture surface, as indicated by arrows. Apparently, those holes were created by the HDPE fiber pullout from the PS matrix and the nodules are broken fiber ends that contracted back after breaking. Since the interfacial adhesion between the PS and HDPE was strong, owing to the SBS layer at the interface, the fiber pullout process would impose a shear stress component on the neighboring PS matrix and promote matrix shear deformation.

Based on the results, it is reasonable to propose that the very high toughness found in the PS/HDPE/SBS ternary blends is a result of the synergistic toughening effect of the HDPE and SBS and the unique microstructure of the ternary blends plays a key role in toughening. Because of the low miscibility between the HDPE and PS, the HDPE forms relative large particles during its blending with the PS in the first step mixing. When the PS/HDPE pre-blend is mixed with the SBS in the second step mixing, the SBS copolymer migrates to and stays at the PS–HDPE interface, because the S-block of the copolymer is miscible with the PS phase and the B-block has relatively high affinity with the HDPE phase. Thus, the HDPE particles will establish reasonably strong adhesion with the PS matrix through the SBS interphase and, meanwhile, maintain relatively large particle size. During the subsequent injection molding process, the large HDPE particles will be converted into long fibers with the SBS coated on the fiber surface.

When a ternary blend with such a microstructure is subjected to an impact loading, a large number of crazes will form in the PS matrix at the beginning of the loading. However, the crazes will soon be stabilized by the neighboring HDPE fibers, which enables the specimen to sustain a higher loading. Although further loading will eventually turn some crazes into cracks and break down the specimen, the HDPE fibers and the strong PS–HDPE adhesion will make the entire fracture process a more difficult one, because the fracture will involve many energy dissipating processes, including craze formation, developing and stabilization; crack initiation, growing and deflection; fiber-matrix debonding, fiber bridging, breaking and pullout. The fiber pullout process, furthermore, will impose a shear stress component on the PS matrix, promoting shear deformation, which is one of the major energy-dissipating events. To summarize the proposed toughening mechanisms, a schematic drawing of the mechanisms is given in Fig. 11a–c.

The direct evidence of the fracture process described in the above text was pursued using a TEM with ultra-thin specimens containing an arrested crack tip. As demonstrated by the TEM micrographs in Fig. 12, a large plastic zone was

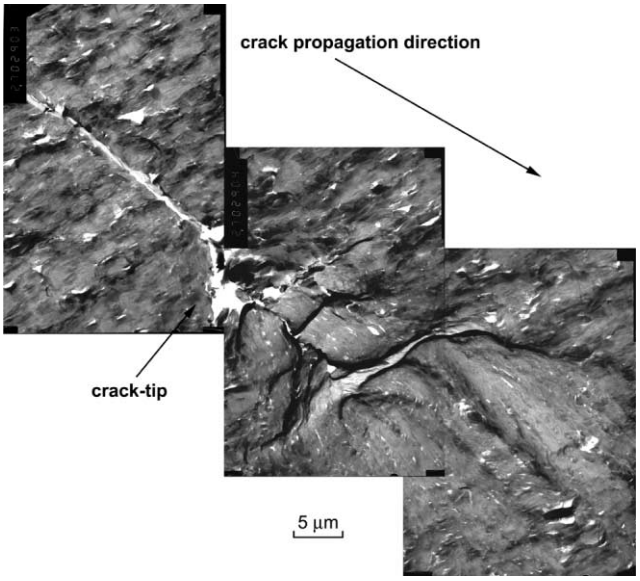

Fig. 12. TEM micrograph taken from an ultra-thin section of the PS/HDPE/SBS (72/18/10) ternary blend, which contains an arrested crack tip and was stained with RuO_4.

formed in front of the arrested crack tip. A large number of cavities, obviously caused by fiber-matrix debonding, can be clearly seen. Extensive shear deformation occurred in both the PS and HDPE phases, although it is difficult to distinguish the two phases on the TEM micrograph. The evidence of HDPE-fiber pullout cannot be found on the micrograph, though we had expected to see a similar fiber pullout picture as those reported in glass or carbon fiber reinforced composites [11]. This can be explained by the fact that the deformed HDPE fibers are very soft and ductile compared with glass and carbon fibers. The HDPE fibers, which had been pulled out of the matrix, would contract back and form nodules, as shown in the SEM micrograph (cf. Fig. 10). It is also possible that the fibers were bended back when the crack surfaces were closed down after unloading. Nevertheless, an enlarged micrograph taken from another specimen of the same blend shown in Fig. 13 clearly demonstrates that even when the crack was propagating in a direction parallel to the fiber alignment direction, the HDPE fibers would still bridge the crack surfaces, which is direct evidence of good PS–HDPE adhesion and fiber bridging toughening.

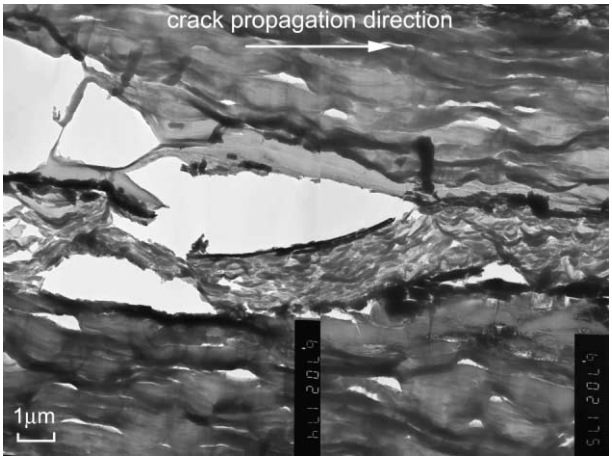

Fig. 13. TEM micrograph of an arrested crack tip showing crack bridging, cavitation and extensive plastic deformation in the PS/HDPE/SBS (72/18/10) ternary blend.

4. Conclusion

The morphology and mechanical properties of the PS/HDPE and PS/SBS binary blends and the PS/HDPE/SBS ternary blends were studied. Based on the results of the work, the following conclusions can be drawn.

1. HDPE formed long fibers in both the PS/HDPE and PS/HDPE/SBS blends. The interfacial bonding between the PS and HDPE was very poor in the binary blends. In the ternary blends, the SBS copolymer formed a thin layer covering the HDPE fibers, resulting in a relatively strong bonding between the HDPE and PS.
2. Due to the high miscibility between the PS and SBS, very fine SBS particles (50–100 nm) were found in the PS/SBS blends.
3. The mechanical properties of both binary blends were poor. The impact strength of the blends decreased with increase of the HDPE or SBS content. The low impact strength for the PS/HDPE blends was very likely due to the poor interfacial adhesion between the PS matrix and HDPE fibers. For the PS/SBS blends, the poor impact strength was caused by the fine SBS particles, which were too small to stabilize the growing crazes and prevent them from developing into cracks.
4. A remarkable enhancement in the impact strength (15 times) was achieved with the PS/HDPE/SBS ternary blends. Mechanism study by the SEM and TEM suggests that the crazes formed in the PS matrix might be stopped by the HDPE fibers, which were strongly bonded to the matrix. Many energy-dissipating processes are therefore involved in the fracture process of the specimen. Among them are fiber-matrix debonding-cavitation, fiber stretching, pullout and bridging and, extensive matrix shear yielding.

Acknowledgements

This work was supported by the Hong Kong Government Research Grant Council under the grant number of HKUST6105/97E and HKUST6033/98P. The authors wish to thank the Advanced Engineering Materials Facility (AEMF) and the Materials Characterization and Preparation Facility (MCPF) of the Hong Kong University of Science

and Technology (HKUST) for their kind support on sample preparation and testing.

References

[1] Bucknall CB. Toughened plastics. London: Applied Science Publishers Ltd, 1977.
[2] Bucknall CB, Smith RR. Polymer 1965;6:437.
[3] Yee AF, Pearson RA. J Mater Sci 1986;21:2462.
[4] Pearson RA, Yee AF. J Mater Sci 1986;21:2475.
[5] Parker DS, Sue H-J, Huang J, Yee AF. Polymer 1990;31:2276.
[6] Yee AF, Olszewski WV, Miller S. Advances in chemistry series, vol. 154. Washington, DC: American Chemical Society, 1976 p. 97.
[7] Yee AF. J Mater Sci 1977;12:757.
[8] Yee AF, Maxwell MA. Polym Eng Sci 1981;21:205.
[9] Sue H-J, Yee AF. J Mater Sci 1989;24:1447.
[10] Wu JS, Yee AF, Mai Y-W. J Mater Sci 1994;29:4510.
[11] Wong S-H, Mai Y-W. Polym Eng Sci 1999;39:356.
[12] Newman S, Strella S. J Appl Polym Sci 1965;9:2297.
[13] Strella S. J Polym Sci 1966;3(A2):527.
[14] Bucknall CB, Clayton D, Keast WE. J Mater Sci 1972;7:1443.
[15] Donald AM, Kramer EJ. J Appl Polym Sci 1982;27:3729.
[16] Wu S. Polymer 1985;26:1855.
[17] Borggreve RJM, Gaymans RJ, Schuijer J, Ingen-Housz JF. Polymer 1987;28:1489.
[18] Wu S. J Polym Sci Polym Phys Ed 1983;21:699.
[19] Hancock M. In: Rothon R, editor. Particulate-filled polymer composites. New York: Longman Group Limited, 1995. p. 279.
[20] Wang K, Wu JS, Kim JK, Zeng HM. In: Ye L, Mai Y-W, editors. Proceedings of International Workshop on Fracture Mechanics and Advanced Materials. University of Sydney, Sydney, 1999. p. 380.
[21] Hobbs SY, Dekkers MEJ, Watkins VH. J Mater Sci 1988;23:1219.
[22] Wu JS, Mai Y-W, Cotterell B. J Mater Sci 1993;28:3373.
[23] Wu JS, Mai Y-W. J Mater Sci 1993;28:6167.
[24] Murff SR, Barlow JW, Paul DR. J Appl Polym Sci 1984;29:3231.
[25] Chung JYJ, Lazear NR, Grigo UR. ANTEC '1985 1985:944.
[26] Lin KP, Chang FC. Polym Networks Blends 1994;4:51.
[27] Liao ZL, Chang FC. J Appl Polym Sci 1994;52:1115.
[28] Wu JS, Mai Y-W. Key Eng Mater 1998;145–149:787.
[29] Wu JS, Pu X, Mai Y-W. Polym Eng Sci 2000;40:786.
[30] Cheng TW, Keskkula HK, Paul DR. Polymer 1992;33:1606.
[31] Takeda Y, Keskkula H, Paul DR. Polymer 1992;33:3394.
[32] Fowler ME, Keskkula H, Paul DR. Polymer 1987;28:1703.
[33] Wang Z, Chan C-M, Zhu S-H, Shen J. Polymer 1998;39:6801.
[34] Liu TM, Evans R, Baker WE. ANTEC '1995 1995:1564.
[35] Liu YH, Zumbrunnen DA. J Metarterioles Sci 1999;34:1921.
[36] Bureau MN, Di Francesco ED, Denault J, Dickson JI. Polym Eng Sci 1999;39:1119.
[37] Xu SA, Tjong SC. Polym J 2000;32:208.
[38] Xu SA, Chan C-M. Polym J 1998;30:552.
[39] Champagne MF, Dumoulin MM. ANTEC '1997 1997:2562.
[40] Chen CC, White J. Polym Eng Sci 1993;33:923.
[41] Wu JS, Chan C-M, Mai Y-W. In: Shonaike GO, Simon GP, editors. Polymer blends and alloys. New York: Marcel Dekker Inc., 1999. p. 505.
[42] Pearson RA, Yee AF. J Mater Sci 1991;26:3828.
[43] Li J-X, Chan C-M, Guo B-H, Wu JS. Macromolecules 2000;33:1022.
[44] Cook DG, Rudin A, Plumtree A. J Appl Polym Sci 1993;48:75.
[45] Moor JD. Polymer 1971;12:478.